Adaptive R-peak Detection Using Empirical Mode Decomposition

Christina Kozia, Randa Herzallah, and David Lowe

Department of Mathematics, Aston University,
Birmingham, United Kingdom
{koziac,r.herzallah,d.lowe}@aston.ac.uk

Abstract. Accurate QRS detection plays a pivotal role in the diagnosis of heart diseases and the estimation of heart rate variability and respiration rate. The investigation of R-peak detection is a continuing concern in computer-based ECG analysis because current methods are still inaccurate and miss heart beats. This paper presents a different algorithm to the state-of-the-art Empirical Mode Decomposition based algorithms for R-peak detection. Although our algorithm is based on Empirical Mode Decomposition, it uses an adaptive threshold over a sliding window combined with a gradient-based and refractory period checks to differentiate large Q peaks and reject false R peaks. The performance of the algorithm was tested on multiple databases including the MIT-BIH Arrhythmia database, Preterm Infant Cardio-Respiratory Signals database and the Capnobase dataset, achieving a detection rate over 99%. Our modified approach outperforms other published results using Hilbert or derivative-based methods on common databases.

Keywords: R-peak detection, Empirical Mode Decomposition, Local Signal Energy

1 Introduction

The QRS complex is of focal interest in computer-based ECG signal analysis as it is the most distinguishable feature of the heart signal and embodies valuable information from which the Heart Rate Variability [1] and Respiration Rate [2] can be estimated. Signal contamination from various types of noise and the variability of the QRS morphology make the detection of the latter more complex. Moreover, the complexity of QRS identification relies on the difficulty in differentiating the R peaks from large P or T peaks [3].

Several methods for QRS detection have been proposed, from derivative based methods [3], [4] to neural networks methods [5], [6]. The majority of the algorithms consist of two stages: pre-processing and decision. The signal is preprocessed in order to enhance the QRS complex and eliminate noise and baseline wander and then a set of thresholds is applied in order to identify the real R peaks in the signal. In [3] and [4] the QRS complex is enhanced by differentiating and then integrating the signal, in order to obtain the slope and width information of the QRS complex. The decision rules are based on estimators of signal

or noise level, such as the mean and the median. In [7] and [8] it was proposed to pre-process the signal using the Hilbert transform of its first derivative. The zero-crossings in the derivative are represented as peaks in the Hilbert sequence. The regions of high probability to identify an R peak are located using a threshold based on the Root Mean Square (rms) of the Hilbert sequence. Finally their method located the real R peaks using a second stage detector based on the heart refractory period (200 milliseconds) [9].

Over the past decade, research in computer-based ECG signal analysis has investigated the use of Empirical Mode Decomposition (EMD) [10] in R peak detection [11], [12], [13]. The EMD method acts as an effective pre-processor which amplifies the QRS complex and decomposes the signal into a set of Intrinsic Mode Functions (IMF). A method of R peak identification by summing the first three IMFs and applying a set of experimentally acquired thresholds was developed in [11]. The reconstruction of the ECG waveform by adding the first three IMFs and then applying a threshold based on 50% of the maximum amplitude was reported in [12] and [13]. The major drawback of [11] and [12] is that they have established an empirical threshold scheme. A serious weakness with the detectors being proposed in [11], [12] and [13] is that the threshold is derived from the full length ECG. Generally difficulties arise when the signal includes very large R peaks, making the threshold high. This results in the failure to detect lower R peaks. Our method provides a solution to detect these lower R peaks by dividing the signal into segments.

Our proposed method for the detection of the QRS complex overcomes the aforementioned problems in the current state-of-the-art EMD methods by introducing an adaptive threshold which is calculated from the local energy of the reconstructed ECG signal from the EMD. The pre-processing stage of our QRS detector contains a band-pass filter in order to eliminate noise and reduce the number of the initial IMFs. The reconstruction of the signal using the EMD method facilitates the removal of low frequency interference and the absolute value of the reconstructed signal amplifies the QRS complexes. The signal is then divided into segments in order to increase the efficiency of the algorithm. Compared with the existing results on the topic, our study has three distinct features that have not been reported in the literature. Firstly, the proposed detector provides a solution for the detection of small R peaks by establishing a threshold derived from the mean of the rms over a prespecified number of most recent segments. Secondly, the threshold established relies on the local signal energy of each segment. Thirdly, the present research explores the differentiation of R peaks from large Q peaks in the absolute value of the signal, by using the first derivative of the ECG signal.

2 Empirical Mode Decomposition

EMD decomposes the signal, $x(t)$, into a series of narrow-band signals, $c_i(t)$, which are called IMFs, and fulfill special conditions. An oscillatory mode of the signal is an IMF exclusively under the conditions that: first, in the whole dataset,

the number of zero-crossings and the number of extrema are either equal or differ at most by one; and second, at any point, the mean value of the maximum and the minimum envelope is zero. The key advantage of EMD is that it is a data-driven analysis method. In each iteration the algorithm needs to decide if the i-th component, $h_i(t)$, extracted from the data, is an IMF based on the conditions mentioned above. In order to achieve this, the EMD method uses a systematic way which is called the *sifting process* and is described as follows: for a given signal $x(t)$, the extrema points are first identified, followed by approximation of the upper, $\widehat{r}(t)$, and lower, $\underline{r}(t)$, envelopes of the signal through a cubic spline interpolation. The mean is then obtained, and the i-th component, $h_i(t)$, is computed as the difference between the signal and the mean. The *sifting process* has to be repeated as many times as required to reduce the extracted signal to an IMF. For our implementation in order to terminate the EMD algorithm, the number of zero-crossings and the number of extrema are checked for equality or whether they differ at most by one. If the final residue, $r_N(t)$, is obtained as a monotonic function, the *sifting process* is stopped, $c_i = h_i$, and the signal, $x(t)$, can be written as follows:

$$x(t) = \sum_{i=1}^{N} c_i(t) + r_N(t) \ , \tag{1}$$

where N is the total number of the extracted IMFs.

3 Proposed R-peak Detection

The proposed algorithm is based on the assumption that the QRS complex of the ECG signal can be enhanced by reconstructing the signal from the first three IMFs of the EMD. This assumption is verified on all of the tested recordings as well be shown in Section 4. However, before applying the EMD, the signal is first processed by a band-pass filter to decrease the computational cost and reduce the number of IMFs. Following the pre-processing stage, the reconstructed signal is divided into a number of segments. Then the envelope of the maxima of each segment is approximated. This is followed by the computation of the local signal energy of each segment and an averaging step for the evaluation of the threshold. Moreover, a few checks were implemented to minimize false positives and negatives including the refractory period and the calculation of the derivative of the ECG signal to discriminate large Q peaks from R peaks in the absolute of the signal. The chosen duration of the segment provides an adequate number of QRS complexes and depends on the sampling frequency. Moreover, for the averaging step the eight most recent segments were used. The number of segments to be averaged is a prespecified parameter which can be decided based on the clinical condition of the patient and whether it is expected that their ECG signal is going to be less or highly variant. However, it is recommended that just the most recent history of the ECG vital signs are kept, thus we used the eight most recent values in the current paper. To summarise, the proposed QRS complex detection algorithm is as follows:

3.1 Pre-processing Stage

1. The raw signal, $x(t)$, is first filtered with a band-pass filter, whose coefficients were designed using a Kaiser-Bessel window [14]. The band-stop frequencies were set at 8 and 20 Hertz [15] in order to amplify the QRS complex, eliminate noise and reduce the number of IMFs. The output of the filter is denoted as $x_f(t)$,
2. The EMD method is applied to $x_f(t)$ to extract the IMFs, $c_1(t) \dots c_N(t)$, where N is the total number of the extracted IMFs,
3. The signal is reconstructed by adding the first three IMFs,

$$x_r(t) = \sum_{i=1}^{3} c_i(t) \ , \tag{2}$$

   where the number of IMFs is experimentally selected and it will be discussed later,
4. Then, the absolute value of the reconstructed signal is computed, that is $a(t) = |x_r(t)|$. This makes all data points positive and implements a linear amplification of the reconstructed signal emphasising the higher frequencies.

3.2 Decision Stage

5. In order to increase the efficiency of the algorithm, we divide $a(t)$ into k segments of 3 seconds duration, that is $k = (\text{total number of samples})/(3 * fs)$. The starting point of the k-th segment should match the last R peak located in the $k-1$ segment in order increase the accuracy,
6. Compute the envelope of the maxima, $\hat{a}_k(t)$, of $a_k(t)$ for each segment k through a cubic spline interpolation of the local maxima,
7. Compute the local signal energy for each segment as,

$$RMS_k = \sqrt{\frac{1}{M} \sum_{t=1}^{M} [\hat{a}_k(t)]^2} \ , \tag{3}$$

   where k is the current segment and M is the number of samples in the segment, that is $M = 3 * fs$,
8. The threshold of the k-th segment is set to be the mean of the most recent eight RMS_k values,

$$T_k = \frac{1}{8} \sum_{j=k-7}^{k} RMS_j \ , \tag{4}$$

9. The peaks, which exceed threshold T_k in the absolute sequence $a_k(t)$, are classified as candidate peaks.
10. In order to segregate large Q peaks from R peaks, we compute the first derivative of $x_r(t)$. Peaks with a negative derivative will be investigated further at the refractory period check given next,
11. Apply a refractory period check when the R-R interval of two adjacent peaks is less than 200 milliseconds. Keep the peak with the maximum amplitude.

4 Results and Discussion

The proposed algorithm is based on the assumption that the range of the frequencies of the first three IMFs of the EMD corresponds to the QRS complex which includes high frequencies in the range 3-40 Hertz [9]. Moreover, P and T wave frequencies are about 0.7-10 Hertz [9], thus in order to enhance QRS complexes, the IMFs that correspond to P and T waves should be discarded. The following discussion shows the validity of this assumption. Fig. 1 shows the filtered ECG signal, $x_f(t)$, of recording 100 from the MIT-BIH Arrhythmia database [16] and its first five IMFs obtained after the EMD algorithm. A Fourier

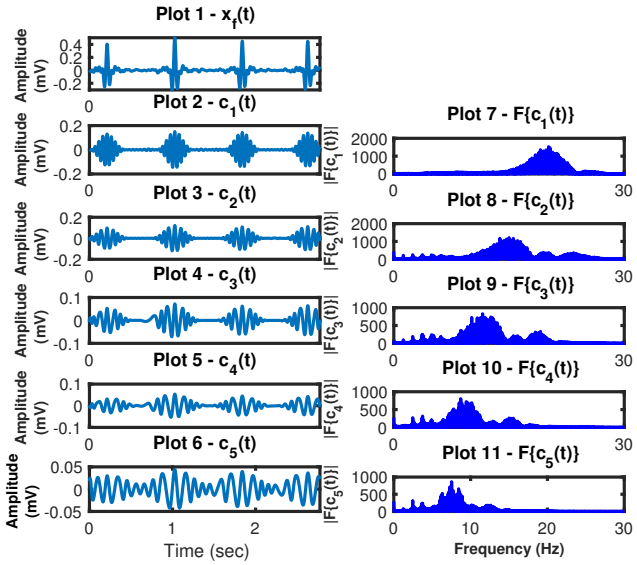

Fig. 1. The result of the EMD and the spectrum of each IMF. Plot 1 corresponds to the filtered ECG, $x_f(t)$. Plots 2 to 6 correspond to the first five IMFs. Plots 7 to 11 correspond to the Fourier transform of each IMF.

transform is applied to each IMF, in order to obtain their frequency bands. It is evident that as the order of the IMFs increases, the frequency content decreases. It can be observed that the spectra of the first three IMFs correspond to the frequency band of the QRS complex. The dominant frequencies in Plots 7-9 (Fig. 1) are about 10-20 Hertz, whereas the dominant frequencies in Plots 10 and 11 are about 2-10 Hertz, which shows that the last two IMFs correspond to P and T waves, hence they should not be used in signal reconstruction. Fig. 2 shows that the filtered signal, $x_f(t)$, can be approximated by the reconstructed signal (summation of the first three IMFs), $x_r(t)$, because the difference of the two signals (red dotted line) is small and the shape of the QRS complex is preserved.

Hence, the first three IMFs are sufficient to delineate the QRS complex. Our

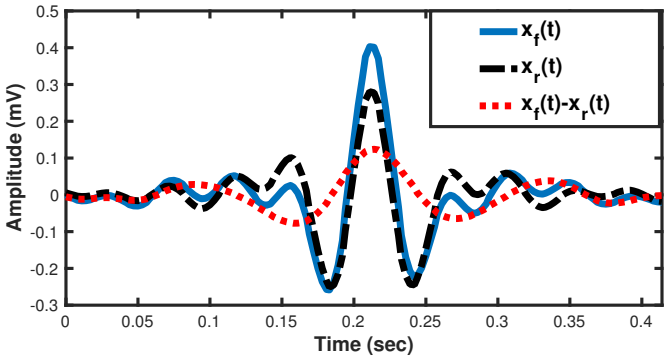

Fig. 2. Reconstruction of the filtered signal, $x_f(t)$, by the summation of the first three IMFs, $x_r(t)$, and their difference, $x_f(t) - x_r(t)$.

assumption was tested on all the recordings under study and the first three IMFs were found to be sufficient for reconstructing the signal, enhance the QRS complex and eliminate low frequency interference. Furthermore, the number of the extracted IMFs for recording MIT-BIH 100 before applying the band-pass filter was 24, and after applying the filter was 22. Following this verification step, our proposed QRS detector was tested using the entire records from the MIT-BIH Arrhythmia database [16] which belong to adults, and all the records from the Preterm Infant Cardio-Respiratory Signals database [16], [17]. Moreover, our method was tested on real data from the Capnobase dataset [18] which were collected during elective surgery and routine anaesthesia and belong to children of ages in ranges 1-14 years old. Furthermore, all databases under study provide annotated R peaks. Fig. 3 shows the sequential steps of the QRS detector. The detected R peaks are marked by an asterisk '*' on the filtered signal, $x_f(t)$ (Plot 4).

For all the databases the results obtained from the proposed method are shown in Table 1, Table 2 and Table 3. Table 4 shows a comparison of our method's performance with other existing methods. A false negative (FN) occurs when the algorithm fails to detect an actual R peak. A false positive (FP) represents a false peak detection. *Sensitivity* (Se), *Positive Predictivity* ($+P$) and *Detection Error Rate* (DER) were calculated using the following formulas respectively:

$$Se(\%) = \frac{TP}{TP + FN}\% \ , \tag{5}$$

$$+P(\%) = \frac{TP}{TP + FP}\% \ , \tag{6}$$

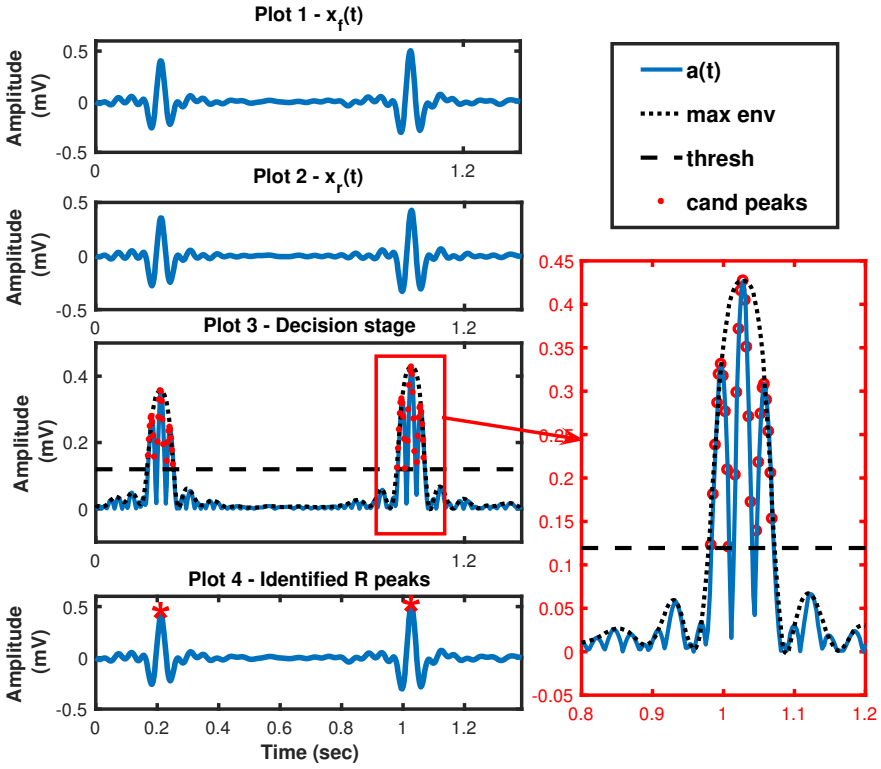

Fig. 3. Steps of the QRS detector for a part of the record 100 from the MIT-BIH database. Plot 1, corresponds to the filtered ECG signal, $x_f(t)$. Plot 2, corresponds to the reconstructed signal, $x_r(t)$. Plot 3, shows the absolute sequence, $a_k(t)$, (blue line) and its maximum envelope, $\hat{a}_k(t)$, (dotted black line) along with the threshold (dashed black horizontal line) and candidate peaks marked with a red asterisk '*'. Plot 4, shows the identified R peaks on $x_f(t)$ as red asterisk '*'.

$$DER(\%) = \frac{FP + FN}{\text{total number of R peaks}}\% \ , \tag{7}$$

where TP (true positives) is the total number of R peaks correctly identified by the detector.

Table 1. QRS detection performance using the MIT-BIH Database

MIT-BIH record	Annotated peaks	DER (%)	*Se* (%)	*+P* (%)
100	2273	0.00	100	100
101	1865	0.48	99.95	99.57
103	2084	0.00	100	100
104	2229	1.57	100	98
105	2572	2.33	99.92	97.79
106	2027	0.98	99.41	99.60
107	2137	0.47	99.81	99.72
109	2532	0.28	99.72	100
111	2124	0.66	99.95	99.39
112	2539	0.20	100	99.80
113	1795	0.11	100	99.89
115	1953	0.00	100	100
117	1535	0.00	100	100
118	2278	0.04	100	99.96
119	1987	0.25	100	99.75
121	1863	0.16	99.95	99.90
122	2476	0.00	100	100
123	1518	0.06	100	99.93
124	1619	0.30	99.81	99.77
Average	35740	0.42	99.92	99.66

As can be seen from Table 4 our method shows a better performance for the MIT-BIH records, achieving higher *Se* of 99.92% compared to 99.86% in [7] and 99.80% in [3] as well as lower DER of 0.42% compared to 14.3% in [7] and 1.33% in [3]. Furthermore, the highest *Se* percentages are reported for PICSDB and Capnobase records by our detector, compared to [3] and [7] (Table 4).

Compared to existing R peak detection methods, the following observations were found. Firstly, during our experiments we observed that some of the adult recordings from the MIT-BIH database include inverted R peaks and this increases the R-peak time-of-occurrence error. The QRS detector fails to detect the inverted R peaks. However, it identifies as a real R peak, a peak close to the inverted one which is not counted as a FP. Hence, the time difference between the actual and the detected peak is large and affects the time-of-occurrence error. Same problem occurs with existing methods [3], [4], [7], [8], [11], [12], [13]. We will further investigate this problem in future research. Secondly, another important observation, which yields high error in the detection of R peaks was seen in some recordings from the MIT-BIH database, is that the absolute am-

Table 2. QRS detection performance using the PICSDB

PICSDB record	Annotated peaks	DER (%)	*Se* (%)	*+P* (%)
infant1	4671	0.08	99.95	99.95
infant2	970	1.34	100	98.70
infant3	1757	0.91	100	99.10
infant4	2300	0.00	100	100
infant5	4434	0.04	100	99.95
infant6	3974	0.30	100	99.70
infant7	4451	0.13	100	99.87
infant8	4185	0.02	100	99.98
infant9	4426	0.59	99.50	99.91
infant10	4572	0.19	100	99.80
Average	15371	0.36	99.95	99.70

Table 3. QRS detection performance using the Capnobase Dataset

Capnobase record	Annotated peaks	DER (%)	*Se* (%)	*+P* (%)
9	815	0	100	100
15	960	0	100	100
16	1012	0	100	100
18	1131	0	100	100
23	818	0	100	100
28	588	0	100	100
29	546	0	100	100
31	539	0	100	100
32	685	0	100	100
35	900	0.18	100	99.89
38	956	0	100	100
103	826	0	100	100
104	912	0	100	100
105	530	0.37	100	99.62
Average	12094	0.03	100	99.97

Table 4. Comparison of QRS detector performance with other methods

Database	Method	DER (%)	*Se* (%)	*+P* (%)
MIT-BIH	Derivative based [3]	1.33	99.80	98.85
	Hilbert transfrom [7]	14.23	99.86	99.71
	Our method	0.42	99.92	99.66
PICSDB	Derivative based [3]	0.34	99.86	99.81
	Hilbert transfrom [7]	0.14	99.92	99.84
	Our method	0.36	99.95	99.70
Capnobase	Derivative based [3]	0.03	100	99.97
	Hilbert transfrom [7]	0.04	100	99.95
	Our method	0.03	100	99.97

plitude of a Q peak is larger than the R peak. This was found to identify the Q peak as a real R peak, because in the decision stage the threshold is applied to the absolute of the reconstructed signal. Fig. 4 shows part of the MIT-BIH 104 record where the absolute amplitude of some of the Q peaks is larger than the R peak. To address this issue the first derivative of the ECG signal is computed. The derivative after an R peak is negative because the signal decreases in time. The derivative after a Q peak is positive as the signal increases in time. Our method was modified and for each candidate peak also the sign of the derivative was checked. Peaks with a negative derivative were investigated further in the decision stage by applying the refractory period check of 200 milliseconds. Hence, the QRS detector proposed in this paper can efficiently distinguish Q from R peaks, whereas existing methods do not propose anything about this issue [12], [13]. Thirdly, current EMD based methods use the average of the mean of all

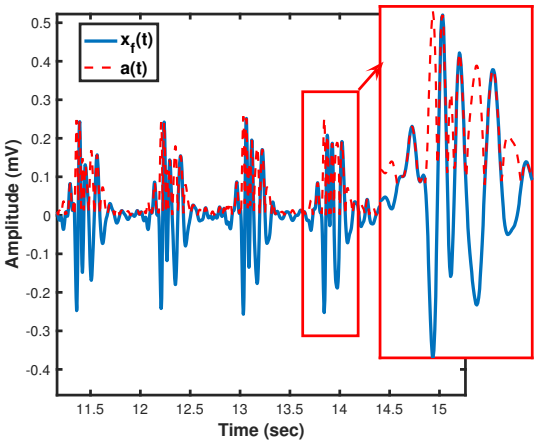

Fig. 4. Part of the filtered ECG signal, $x_f(t)$, and its absolute value, $a(t)$, from the MIT-BIH 104 record. The dashed line in the red box shows that the absolute amplitude of the Q peak exceeds the amplitude of the R peak.

segments [12] and 0.5 of the maximum amplitude [13] to calculate the threshold. When we computed these thresholds for recording MIT-BIH 104, we found the threshold of 0.5 of the maximum amplitude [13] to be high, about 0.5161, while the average of the mean [12] is found to be very low, about 0.0847, thus producing large number of FPs and FNs. Our threshold computed as the average of the rms over the full record was found to be 0.1153, thus minimising FPs and FNs. This is shown in Fig. 5 where as can be seen our peak detector, Fig. 5. Plot 2, has identified all R peaks correctly while the 0.5 of the max amplitude threshold [13], misses too many peaks as can be seen from Fig. 5. Plot 1.

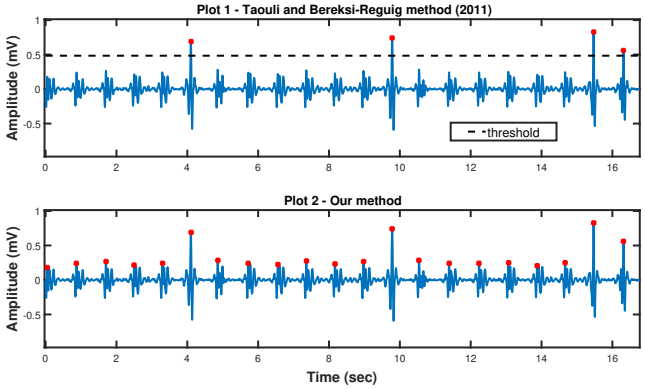

Fig. 5. Plot 1 shows the detected R peaks for a part of MIT-BIH 104 record using the method proposed in [13]. Plot 2 shows the detected R peaks for the same part of ECG using the proposed method.

5 Conclusion

To conclude, a new QRS detector was presented based on Empirical Mode Decomposition using an adaptive threshold which relies on the local signal energy. Our method provides a solution for the detection of small R peaks by establishing a threshold derived from the mean of the rms over eight segments. In addition, our detector correctly discriminates R peaks from large Q peaks in the absolute value of the signal, by using the first derivative of the ECG signal. Using the MIT-BIH Arrhythmia database, the method performed effectively with accurate QRS complex detection of 99.92%, using the Preterm Infant Cardio-Respiratory Signals database and using the Capnobase dataset the method performed effectively with an Se of 99.95% and 100%, respectively. The proposed method shows comparable results with other published methods using derivative-based [3] and Hilbert methods [7] on common databases and real data. However, the average R-peak time-of-occurrence error remains an issue to be addressed, thus the problem of the inverted R peaks is going to be part of our future work.

Acknowledgments. This work is supported by Isansys Lifecare Ltd.

References

1. Moody, G. B.: Spectral analysis of Heart Rate without resampling. Computers in Cardiology, 715-718 (1993)
2. Moody, G. B., Mark, R. G., Zoccola, A., Mantero, S.: Derivation of respiratory signals from multi-lead ECGs. Computers in Cardiology, 113-116 (1985)
3. Pan, J., Tompkins, W. J.: A real-time QRS detection algorithm. IEEE transactions on Biomedical Engineering 3, 230-236 (1985)

4. Hamilton, P. S., Tompkins, W. J.: Quantitative investigation of QRS detection rules using the MIT/BIH Arrhythmia database. IEEE transactions on Biomedical Engineering 12, 1157-1165 (1986)
5. Maglaveras, N., Stamkopoulos, N., Diamantaras, T., Pappas, T., Strintzis, M.: ECG pattern recognition and classification using non-linear transformations and neural networks: A review. International journal of Medical Informatics 52(1), 191-208 (1998)
6. Kohler, B. U., Hennig, C., Orglmeister, R.: The principles of software QRS detection. IEEE Engineering in Medicine and Biology Magazine 21(1), 42-57 (2002)
7. Benitez, D. S., Gaydecki, P. A., Zaidi, A., Fitzpatrick, A. P.: A new QRS detection algorithm based on the Hilbert transform. Computers in Cardiology 27, 379-382 (2000)
8. Benitez, D. S., Gaydecki, P. A., Zaidi, A., Fitzpatrick, A. P.: The use of Hilbert transform in ECG signal analysis. Computers in Cardiology and Medicine 31(5), 399-406 (2001)
9. Malmivuo, J., Plonsey, R.: Bioelectromagnetism: Principles and Applications of Bioelectric and Biomagnetic fields. Oxford University Press (1995)
10. Huang, N. E., et al.: The Empirical Mode Decomposition and the Hilbert spectrum for nonlinear and non-stationary time series analysis. Proceedings of the Royal Society of London A: Mathematical, Physical and Engineering Sciences 454, 903-995 (1998)
11. Yang, X. L., Tang, J. T.: Hilbert-Huang transform and Wavelet transform for ECG detection. 4th International Conference on Wireless Communications, Networking and Mobile Computing, WiCOM'08, 1-4 (2008)
12. Arafat. M. A., Hasan, M. K.: Automatic detection of ECG wave boundaries using Empirical Mode Decomposition. ICASSP, IEEE International Conference on Acoustics, Speech and Signal Processing, 461-466 (2009)
13. Taouli, S., Bereksi-Reguig, F.: Detection of QRS complexes in ECG signals based on Empirical Mode Decomposition. Global Journal of Computer Science and Technology 11(20) (2011)
14. Proakis, J. G., Manolakis, D. G.: Digital Signal Processing: principles, algorithms, and applications (3rd edition). Prentice hall (1996)
15. Elgendi, M., Jonkman, M., DeBoer, F.: Frequency bands effects on QRS detection. 3rd International Joint Conference on Biomedical Engineering Systems and Technologies (BIOSIGNALS) 5, 428-431 (2010)
16. Goldberger, A. L., et al.: Components of a New Research Resource for Complex Physiologic Signals, PhysioBank, PhysioToolkit, and Physionet, American Heart Association Journals. Circulation 101(23), 1-9 (2000)
17. Gee, A. H., Barbieri, R., Paydarfar, D., Indic, P,: Predicting Bradycardia in Preterm Infants Using Point Process Analysis of Heart Rate. IEEE Transactions on Biomedical Engineering 64(9), 2300-2308 (2017)
18. Karlen, W., Raman, S., Ansermino, J. M., Dumont, G. A.: Multiparameter respiratory rate estimation from photoplethysmogram. IEEE Transactions on Bio-medical Engineering 60(7), 1946-1953 (2013)